Precision Measurement System for the Calibration of Phasor Measurement Units

Dimitrios Georgakopoulos, *Senior Member, IEEE*, and Stephen Quigg

***Abstract*— Phasor measurement units (PMUs) are used for monitoring, protection, and control of smart grids. Characterization of PMUs to national standards of measurement is important to assure reliability and consistency of PMUs across the industry and is required by documentary standards. At the National Measurement Institute, Australia, we have developed a calibration system to provide some calibration points for the characterization of PMUs under steady-state conditions that can be compatible with standard tests. This paper describes the operation and calibration of the system with emphasis on traceability to national standards of measurement.**

***Index Terms*— Electrical measurements, global positioning system (GPS)-related electrical measurements, measurement, measurement standards, phasor measurement units (PMUs), synchronized measurements.**

I. Introduction

PHASOR measurement units (PMUs) are used for monitoring, protection, and control of smart grids. They measure a number of physical quantities based on sampled voltage and current waveforms. The measurement is synchronized to Coordinated Universal Time (UTC) using timing signals that are derived from the global positioning system (GPS) and/or other Global Navigation Satellite Systems [1]. Consistent performance of PMUs, installed, operated, and maintained by different entities, is fundamental for the successful deployment of PMUs and is an ongoing research and development activity as the power industry transitions from traditional to modern power grid technologies [2]. It is achieved by ensuring conformance with documentary standards that specify the measurement requirements of PMUs (see [1]), and through traceability of the corresponding measurement to the international system of units realized by the national standards of measurement.

Development of facilities for the calibration of PMUs is currently an area of increasing effort (see [2]–[7]). At the National Measurement Institute, Australia (NMIA), we have developed a system for the calibration of PMUs at 50 Hz power system frequency. The purpose of the system is to provide some calibration points that can be compatible with some of the steady-state tests described in [1] at 50 Hz for PMUs deriving their timing from GPS signals. This paper, which is an extension of [8], describes the facility that has been developed at the NMIA, for the calibration of PMUs under steady-state conditions traceable to the national standards of Australia, and reports on its evaluation.

Manuscript received October 12, 2016; accepted November 30, 2016. Date of publication February 1, 2017; date of current version May 10, 2017. The Associate Editor coordinating the review process was Dr. Branislav Djokic.

D. Georgakopoulos is with the Electricity Section, National Measurement Institute, Lindfield, NSW 2070, Australia (e-mail: dimitrios.georgakopoulos@measurement.gov.au).

S. Quigg is the with the Electricity Section, National Measurement Institute, Lindfield, NSW 2070, Australia (e-mail: stephen.quigg@measurement.gov.au).

Color versions of one or more of the figures in this paper are available online at http://ieeexplore.ieee.org.

Digital Object Identifier 10.1109/TIM.2017.2653518

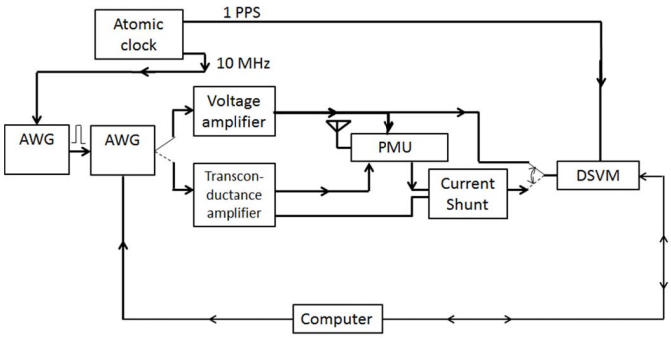

Fig. 1. Block diagram of the NMIA PMU calibration system.

II. System Description

A PMU measures the instantaneous values of magnitude and phase of voltage and current in the form of a synchrophasor (a complex representation of a sinusoidal function) referenced to UTC. A PMU usually has a GPS-disciplined oscillator that generates a 1 pulse per second (1 PPS) timing signal that is referenced to UTC via GPS timing. The rising edge of the 1 PPS signal defines the measurement epoch with the convention that the phase of the synchrophasor is 0° when the rise of the 1 PPS coincides with the cosine of its argument and −90° when the 1 PPS coincides with the sine.

The steady-state tests described in IEEE Std C37.118.1 [1] require the measurement of the total vector error (TVE), a nonlinear function of the real and the imaginary parts of the synchrophasor, the frequency error (FE), and the rate of change of FE (RFE). The measurement of these parameters is based on the measurement of voltage and current signals.

The calibration system is shown schematically in Fig. 1. Two arbitrary waveform generators (AWGs) (Agilent 33210A*) are used to generate one voltage signal with peak value up to 10 V and adjustable phase, based on digital synthesis techniques, with the total harmonic distortion less than 0.02%. The phase of AWG_2 can be adjusted with respect to a trigger signal generated by AWG_1. For the voltage waveform, the output voltage of AWG_2 is amplified to the appropriate voltage level, is connected to the PMU, and is simultaneously measured by a digital sampling voltmeter (DSVM), Agilent 3458A. For the current

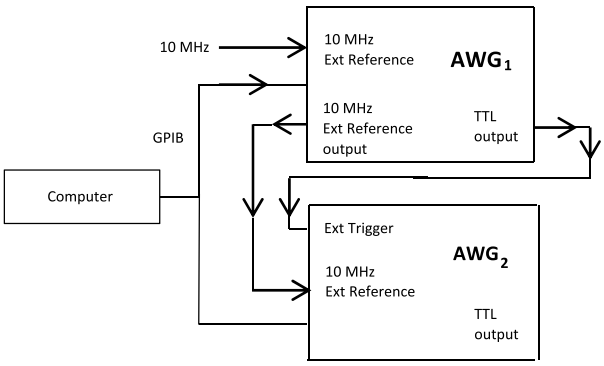

Fig. 2. Detailed triggering arrangement of the AWG.

waveform, the output of AWG_2 is converted into current by a transconductance amplifier and is simultaneously measured by a current shunt and a DSVM. The switches shown in Fig. 1 are not physically present and are only drawn to demonstrate the principle; in practice, the connections are hardwired. The computer shown in Fig. 1 is used for control and data analysis of the NMI PMU calibration system and to collect the data from the PMU under test.

The developed PMU calibration system is single phase and can be used to calibrate PMUs that derive their timing from GPS signals. The GPS antenna used in the system is connected to the PMU under test with a 30 m cable that introduces a nominal time delay of 119 ns. This time delay is not taken into account in the calculations but is reported in the calibration report. The calibration system can use the GPS antenna and the cable of the PMU under test if required, given that the connecting cable is greater than 10 m.

The system timing of the AWG and the measurement are synchronized to our realization of UTC, UTC(AUS). The synchrophasor estimate is referenced on UTC using published corrections for the difference between UTC and UTC(AUS). The synchronization is based on a 10 MHz clock signal and a 1 PPS timing signal that are obtained from a cesium primary standard (Symmetricom 5071A) that is designated as the national frequency standard (NFS). The AWGs are locked to the NFS 10 MHz reference (Fig. 2). The DSVM sampling is synchronized to UTC by the 1 PPS signal. The 1 PPS signal is connected to the external trigger input of the DSVM by a coaxial cable. All the uncertainties given in this paper are expanded uncertainties with a coverage factor of $k = 2.0$.

The DSVM is set to 18-b resolution at a sampling rate of 50 kHz. The DSVM operates in direct sampling dc mode. The current shunts are designed and manufactured at NMIA and have been described in [9].

The traceability of the system is derived from the NFS 10 MHz reference, the difference between UTC and UTC(AUS), the metrological characterization of the DSVM for magnitude and phase, and the current shunt. The uncertainties due to the NFS 10 MHz clock and the difference between UTC and UTC(AUS) are a few parts in 10^9, which are negligible for the characterization of PMUs.

The cable connecting the 1 PPS signal to the external trigger input of the DSVM has a time delay of (662.8 ± 0.5) ns. This time delay is compensated in the software used for data analysis, and its uncertainty is part of the uncertainty analysis.

For all the physical quantities of interest [magnitude and phase of current and voltage, frequency, and rate of change of frequency (ROCOF)], the uncertainty is mainly due to the DSVM. The sampling issues of the DSVM used in the NMIA calibration system are well understood, especially for magnitude, and are described elsewhere (see [10]–[12]). In this paper, we concentrate on the phase errors.

The DSVM introduces a number of time delays in both the analog signal of interest and the 1 PPS used to synchronize the sampling to the UTC. For example, in the digital part of the DSVM, there is a time delay between the external trigger input of the DSVM and the actual time when the analog-to-digital conversion starts due to the impedance of the digital input of the DSVM and its internal circuitry. The uncertainty of the digital trigger level set for sampling the analog signal introduces additional errors in the sampling of the analog signal. The timing errors of the sampling mechanism of the DSVM also introduce errors in both the magnitude and phase of the sampled signal. In the analog part, there is a time delay between the signal input of the DSVM and the analog-to-digital converter due to the signal conditioning electronics (e.g., amplifiers and voltage transducers). The sampling of an analog signal at a specific sampling rate also introduces a sinc function error due to the zero-order hold effect [10]. This sinc function error is corrected in the software used for data processing.

The combined effects of all these errors are quantified for magnitude and phase by calibrating the system at specific points and are compensated using the corresponding corrections during the operation of the system. Hence, the uncertainty components for magnitude and phase are mainly due to the calibration uncertainty of the DSVM for magnitude and phase. For phase, the DSVM is calibrated at 0°, 30°, 60°, and 90° and linear interpolation between the corrections of these calibration points is used for correcting the phase errors of the DSVM at all other points in the data analysis software (see the discussion in Section III).

The voltage and current signals are generated using time domain techniques. For the measurement of TVE and frequency, sinusoidal waveforms are downloaded to the AWG. The magnitude, phase, and frequency are then set by programming the AWG.

For the measurement of the ROCOF, a frequency modulated sinusoidal signal

$$v_{FM} = A\cos\left(\omega_c t + k_f \int m(\tau)d\tau\right) \tag{1}$$

is generated and downloaded to the AWG. At present, as $m(\tau)$ we use only $m(\tau) = (((t + |t|)/2) - A)k_f$, $0 \le t \le ((A(k_f + 1)/k_f)$ (A and k_f are shown in Fig. 3), but other $m(\tau)$ can also be generated.

The measurements of magnitude and phase of the voltage and current signals are based on Fourier analysis [fast Fourier transform (FFT)], as it provides directly the real and imaginary parts of the signal of interest (voltage and current) required for the calculation of the TVE. An integer number of samples per cycle and an integer number of cycles are used in the FFT to eliminate leakage and enable a rectangular window

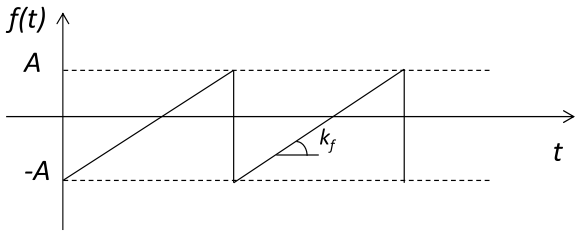

Fig. 3. Frequency modulated signal for the characterization of the PMUs.

to be used for the FFT. From the sampled data collected by the DSVM, the frequency and the ROCOF are measured using a linear interpolation-based zero crossing algorithm, since this algorithm is simple, can be directly related to the frequency standards on a cycle-by-cycle basis, and can be used with frequency modulated signals with noncontinuous frequency modulation.

The linear interpolation-based zero crossing algorithm includes the following steps:

1) from the data collected by the DSVM remove the dc offset of the waveform;
2) search for the zero crossing points of the waveforms;
3) perform linear interpolation on the points around the zero crossing point found in step 2 to estimate the zero crossing point;
4) calculate the frequency of the signal.

Close to the zero crossing points, the approximation $\sin(x) \approx x$ can be used, allowing linear interpolation. The use of this algorithm can give results within a maximum relative error, ε, when the number of samples for each period satisfies $N \geq 2\pi/(6\varepsilon)^{1/2}$.

The linear interpolation-based zero crossing algorithm is suitable for low noise and low distortion sinewaves (e.g., distortion less than 0.1%). Distortion and noise coupled on the measured voltage or current waveform can limit the accuracy of the algorithm. Filtering can reduce the amount of the distortion of the signal of interest to the appropriate level, if necessary. In the NMIA PMU calibration system, the distortion of the voltage and current signals is very low (less than 0.02%) and filtering is not used. Averaging of the estimated frequencies over a number of periods is used to reduce the effect of noise on the performance of the algorithm. The algorithm is particularly useful for providing traceability for the ROCOF, since it is directly traceable to the national standard of frequency because it can estimate the mean frequency for each cycle of the frequency-modulated signal based only on timing information.

III. System Evaluation

The PMU calibration system was evaluated for TVE, FE, and RFE. The evaluation of the TVE requires the metrological characterization of magnitude and phase for both the voltage and the current. The measurement of the FE is straightforward, whereas the measurement of the RFE is the most challenging measurement.

For the voltage TVE characterization, the PMU calibration system was calibrated for voltage by means of a transfer standard (Fluke 5729A) of known ac–dc difference (Table I).

TABLE I
Voltage Calibration of the PMU Calibration System

Magnitude (V)	Correction (μV/V)	Uncertainty (μV/V)
120	− 19	± 65
240	+ 27	± 58

TABLE II
Current Calibration of the PMU Calibration System

Magnitude (A)	Correction (μA/A)	Uncertainty (μA/A)
1	− 16	± 64
10	+ 25	± 72

The magnitude measurements for ac current are traceable to the standard of ac voltage through the transfer standard and to the standard of resistance through the current shunt of known ac–dc difference (Table II).

The phase of the ac voltage measurement is traceable to NMIA power standards by means of a phase reference standard (Clarke-Hess PM5500) used as a transfer standard. The PM5500 produces two sinewave signals (reference and variable) with an adjustable phase angle between them and a resolution of 0.001°. It also produces a TTL signal derived from the reference sinewave. The PM5500 used in this test was modified so that its clock signal was derived from a signal generator referenced to the NFS 10 MHz.

The phase reference standard was calibrated against a power standard for power factor [13]. The external trigger of the DSVM was connected to the TTL output of the PM5500. The expanded uncertainty of this calibration is less than 0.002°, which is dominated by the resolution of the PM5500 (0.001°, rectangular distribution) and the phase uncertainty of [13] for measuring the power between a sinewave and a pulse (better than 0.0015°, Gaussian distribution). This calibration was confirmed using two different techniques, time interval calibration using a counter with calibrated time base and a lock-in amplifier.

The PM5500 cannot generate voltages with an rms value of 240 V, which are required for the calibration of PMUs operating in 240 V power systems. For this reason, the DSVM was calibrated for phase error using the PM5500 both at high voltage for 120 V operation (with the DSVM set to its 1000 V range) and at low voltage (with the DSVM set to its 10 V range). For operation at 240 V, an inductive voltage divider (IVD) with negligible phase error, designed and manufactured at NMIA [14], was used to scale the 240 V to a voltage level less than 7 V rms and the DSVM was set to its 10 V range, which was calibrated against the PM5500.

To obtain confidence in the phase characterization of the DSVM, the phase of a 120 V voltage signal was measured using the DSVM set to two different ranges. A voltage of 120 V magnitude was first applied from the PM5500 to the DSVM that was set to its 1000 V range; then the same voltage was applied to the DSVM set to its 10 V range through the NMIA IVD. Fig. 4 shows the voltage phase correction for various phases at 120 V for two different DSVM

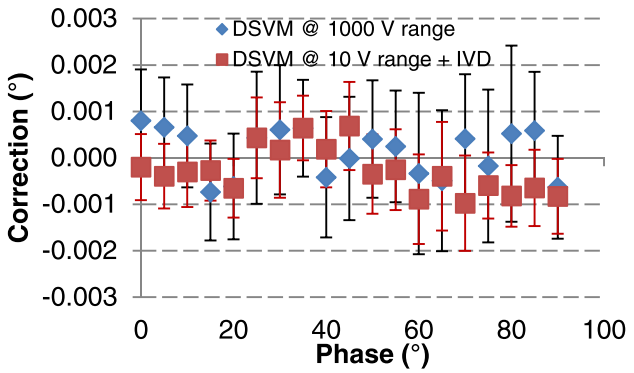

Fig. 4. Phase characterization of the PMU calibration system at 120 V.

configurations. The results agree within their uncertainties, which are better than 0.002°. This uncertainty of the phase includes the variability of the internal time delay of the DSVM. At a phase of 90°, the correction of the DSVM at 240 V was −0.0015° and at 120 V it was −0.0006°. In both the cases, the uncertainty was less than 0.002°.

For these test conditions, in terms of TVE, for voltage magnitude and phase uncertainties of 58 μV/V (Table I) and 0.002°, respectively, the corresponding error in TVE is 0.004%. The phase corrections for the current shunts are referenced to calculable micropotentiometer resistors [15]. The linear interpolation-based zero crossing algorithm for the measurement of frequency was evaluated using both simulated signals with well-defined properties and experimentally.

For the simulation, first, the algorithm was tested with an ideal sinusoidal signal of 25 000 points over 50 periods at a frequency of 50 Hz with rms value of 1 V. For the ideal sinusoidal case, the error of the algorithm was within the numerical error of the computation, better than five parts in 10^{15}. Then the algorithm was tested with a noisy signal consisting of noise with rms value of 140 μV having uniform probability density function superimposed on the ideal sinewave of the first test. The noisy signal was generated using the random generator of L'Ecuyer described in [16]. This algorithm produces pseudorandom sequences with low correlation between successive numbers by combining two different sequences of pseudorandom numbers with different periods to create a new sequence whose period is the least common multiple of the two periods. In this case, the relative difference of the frequency estimated from the algorithm using this noisy sinusoidal signal and the frequency of the ideal sinewave was 1 nHz/Hz with a relative standard error of 400 nHz/Hz. Next, the algorithm was tested with a noisy signal consisting of noise with rms value of 140 μV having Gaussian probability density function superimposed on the ideal sinewave of the first test. The Gaussian random number generator uses the Box–Muller transform [17], which is based on a simple transformation of two sequences of pseudorandom numbers having uniform distribution (such as those generated by the L'Ecuyer algorithm) to produce a sequence of pseudorandom numbers with Gaussian distribution. The relative difference in the frequency estimated from the algorithm for this signal and the frequency of the ideal sinewave was 85 nHz/Hz, with a relative standard error better than 400 nHz/Hz.

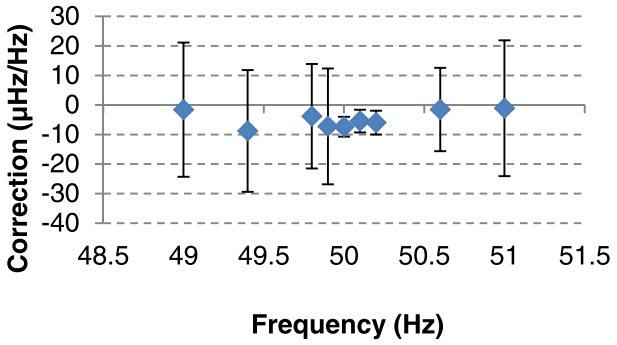

Fig. 5. Static frequency characterization of the PMU calibration system.

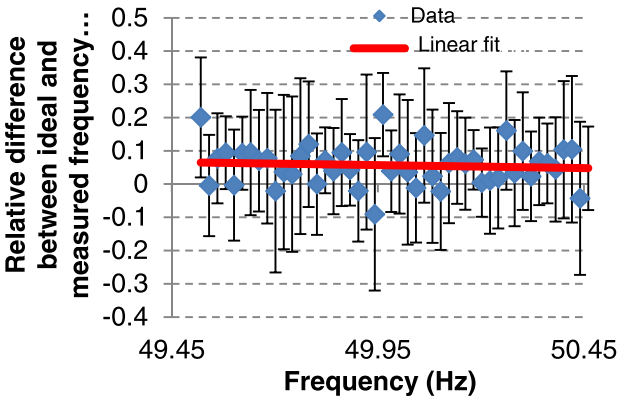

Fig. 6. ROCOF characterization of the PMU calibration system for 1 Hz/s.

TABLE III
RATE OF CHANGE OF FREQUENCY (ROCOF)

ROCOF (Hz/s)	Correction (mHz/Hz)	Uncertainty (mHz/Hz)
0.5	+ 0.7	± 1.7
1	− 0.8	± 1.7

Experimentally, the system was evaluated for frequency using a counter (Agilent 53131A) as transfer standard with a calibrated time base. The system was calibrated for frequencies in the range 45–55 Hz with an uncertainty better than 22 μHz/Hz. The maximum correction of the frequency was better than 10 μHz/Hz. Fig. 5 shows the results for the frequency range 49–51 Hz. The uncertainty is the smallest for frequencies close to 50 Hz and increases as the signal frequency deviates from 50 Hz.

For the ROCOF, traceability was established by referencing the two AWGs to the NFS 10 MHz and measuring the frequency with the DSVM over a number of periods to estimate the ROCOF. Table III shows the results for a ROCOF of 0.5 and 1 Hz/s. These results were confirmed using a counter to measure the frequency for a large number of periods and using the statistical functions of the counter to find the maximum and minimum values of the frequency. Fig. 6 shows the relative difference between the ideal and measured frequency for different frequencies of the frequency modulated signal with a ROCOF of 1 Hz/s and the corresponding linear least squares fit. Table IV shows a typical uncertainty budget for the ROCOF. The largest uncertainty component is that of the unit under test.

TABLE IV
TYPICAL UNCERTAINTY BUDGET FOR THE ROCOF

Component	Value (mHz/Hz)	Divisor	Standard uncertainty	Sensitivity factor	Contribution to uncertainty $u(y_i)$	Degrees of freedom (ν_i)	$u(y_i)^2$	$u(y_i)^4/\nu_i$
Reference (Agilent 3458A)	0.03	2	0.02	1	0.02	1000	0.00	0.0
Algorithm	0.00004	2	0.00	1	0.00	2	0.00	0.0
UUT resolution	1.00	1.73	0.58	1	0.58	1000	0.33	0.0
Rounding of result	0.10	1.73	0.06	1	0.06	1000	0.00	0.0
Type A (3458A)	0.10	1	0.10	1	0.10	9	0.01	0.0
Type A (UUT)	1.00	1.73	0.58	1	0.58	9	0.33	0.0
				Combined standard uncertainty	0.8 mHz/s			
				Effective degrees of freedom	37.2			
				Coverage factor (for 95% level of confidence)	2.026			
				Expanded uncertainty	1.7 mHz/s			

* The commercial instruments are identified in this paper only in order to adequately specify the experimental procedure. Such identification does not imply recommendation or endorsement by the National Measurement Institute, Australia, nor does it imply that the equipment identified is necessarily the best available for the purpose.

During the development of the system, we have tested one commercial PMU. It was found that this PMU met its specifications for the tested points.

IV. CONCLUSION

We have developed a system for the steady-state calibration of PMUs traceable to the Australian national standards of measurement. The measurement is based on Fourier analysis for magnitude and phase and on a linear interpolation-based zero crossing algorithm for the frequency and the ROCOF. Simulations and experiments were performed to evaluate the PMU calibration system and establish its traceability to the Australian national standards.

ACKNOWLEDGMENT

The authors would like to thank Dr. I. Budovsky for the valuable discussions and for supporting this paper and Dr. M. Wouters for the valuable comments.

REFERENCES

[1] *IEEE Standard for Synchrophasor Measurements for Power Systems*, IEEE Standard C37.118.1, 2011.
[2] D. Novosel, V. Madani, B. Bhargawa, K. Vu, and J. Cole, "Dawn of the grid synchronization," *IEEE Power Energy Mag.*, vol. 6, no. 1, pp. 49–60, Jan./Feb. 2008.
[3] Y.-H. Tang, G. N. Stenbakken, and A. Goldstein, "Calibration of phasor measurement unit at NIST," *IEEE Trans. Instrum. Meas.*, vol. 62, no. 6, pp. 1417–1422, Jun. 2013.
[4] J.-P. Braun and S. Siegenthaler, "Calibration of PMUs with a reference grade calibrator," in *CPEM Conf. Tech. Dig.*, Aug. 2014, pp. 678–679.
[5] U. Pogliano, B. Trichera, and D. Serazio, "A system for the accurate characterization of wideband wattmeters, power quality analyzers and PMUs," in *CPEM Conf. Tech. Dig.*, Aug. 2014, pp. 406–407.
[6] G. A. Kyriazis, W. G. K. Ihlenfeld, and R. P. Landim, "Combined AM and PM signal analysis with applications to the dynamic testing of phasor measurement units," in *CPEM Conf. Tech. Dig.*, Aug. 2014, pp. 682–683.
[7] G. Rieveld, J.-P. Braun, P. S. Wright, P. Clarkson, and N. Zisky, "Smart grid metrology to support reliable electricity supply," in *CPEM Conf. Tech. Dig.*, Aug. 2014, pp. 680–681.
[8] D. Georgakopoulos and S. Quigg, "Precision measurement system for the calibration of phasor measurement units," in *CPEM Conf. Tech. Dig.*, Jul. 2016, pp. 1–2.
[9] I. Budovsky, "Standard of electrical power at frequencies up to 200 kHz," *IEEE Trans. Instrum. Meas.*, vol. 58, no. 4, pp. 1010–1016, Apr. 2009.
[10] W. G. K. Ihlenfeld, "Maintenance and traceability of AC voltage by synchronous digital synthesis and sampling," PTB, Braunschweig, Germany, Tech. Rep. E-75, 2001.
[11] U. Pogliano, "Precision measurement of AC voltage below 20 Hz at IEN," *IEEE Trans. Instrum. Meas.*, vol. 46, no. 2, pp. 369–372, Apr. 1997.
[12] R. Lapuh, B. Voljč, and M. Z. Lindič, "Evaluation of Agilent 3458A time jitter performance," *IEEE Trans. Instrum. Meas.*, vol. 64, no. 6, pp. 1331–1335, Jun. 2015.
[13] G. B. Gubler and E. Z. Shapiro, "Implementation of sampling measurement system for new VNIIM power standard," in *CPEM Conf. Tech. Dig.*, Jul. 2012, pp. 294–295.
[14] G. W. Small, I. F. Budovsky, A. M. Gibbes, and J. R. Fiander, "Precision three-stage 1000 V/50 Hz inductive voltage divider," *IEEE Trans. Instrum. Meas.*, vol. 54, no. 2, pp. 600–603, Apr. 2005.
[15] I. Budovsky, "Measurement of phase angle errors of precision current shunts in the frequency range from 40 Hz to 200 kHz," *IEEE Trans. Instrum. Meas.*, vol. 56, no. 2, pp. 284–288, Apr. 2007.
[16] W. H. Press, S. A. Teukolsky, W. T. Vetterling, and B. P. Flannery, *Numerical Recipes*. New York, NY, USA: Cambridge Univ. Press, 2007.
[17] G. E. Box and M. E. Muller, "A note on the generation of random normal deviates," *Ann. Math. Statist.*, vol. 29, no. 2, pp. 610–611, 1958.

Dimitrios Georgakopoulos (A'11–M'12–SM'12) was born in Athens, Greece, in 1972. He received the B.Eng. degree in electrical engineering from the Technological Educational Institution of Piraeus, Egaleo, Greece, in 1996, the M.Sc. degree in electronic instrumentation systems from the University of Manchester, Manchester, U.K., in 1999, and the Ph.D. degree in electrical engineering and electronics from the University of Manchester Institute of Science and Technology, Manchester, in 2002.

From 2002 to 2007, he was a Research Scientist at the National Physical Laboratory, Teddington, U.K. In 2007, he joined the National Measurement Institute, Lindfield, NSW, Australia, as a Research Scientist, where he has been involved in the development of quantum voltage standards and low frequency electromagnetic compatibility standards.

Dr. Georgakopoulos is a member of the Measurements in Power Systems IEEE Committee (TC-39) and the American Association for the Advancement of Science, USA.

Stephen Quigg, photograph and biography not available at the time of publication.